GEOPHYSICAL RESEARCH LETTERS, VOL. 28, NO. 14, PAGES 2683-2686, JULY 15, 2001

Historical and future trends of the Sahara Desert

Ping Liu

Laboratory of Atmospheric Sciences and Geophysical Fluid Dynamics, Beijing, China

Warren M. Washington and Gerald A. Meehl

National Center for Atmospheric Research, Boulder, Colorado

Guoxiong Wu

Laboratory of Atmospheric Sciences and Geophysical Fluid Dynamics, Beijing, China

Gerald L. Potter

Program for Climate Model Diagnosis and Intercomparison, Livermore, California

Abstract. The Parallel Climate Model (PCM) Version 1.1 simulates a reasonable twentieth century climatology in the Sahara Desert. From late 1940s to the end of 1980s, the simulated Sahara Desert, bounded by the 50 mm mean annual rainfall isoline, becomes larger and shifts eastward. The model produces a decreasing rainfall trend while the surface temperature and meridional boundaries are almost stable. In the usual scenario with increasing greenhouse gases from the 1980s to the 2090s the Sahara becomes smaller, moves north and west and continues to dry. Both the size change and latitudinal shift show a century long trend. Compared to 1961-90 climatology, the average northward shift is around 1° and the surface temperature about 2.8°C warmer to the end of 21^{st} century. The local greenhouse effect may cause such warming trend.

1. Introduction

The Sahara Desert has been expanding southward and contracting northward and getting drier, then wetter from the distant past to modern times [*Maley*, 1977; *Dumont*, 1978; *Ritchie et al.*, 1985; *Gasse et al.*, 1990]. Before the 1970s, the southern boundary displayed a series of decade long drought [*Klaus*, 1978; *Littmann*, 1991] without an established trend or periodicity in the western region [*Bunting*, 1976]. The 1980s brought an apparent expansion and an increase in interannual variations [*Tucker et al.*, 1991].

The southern Sahara Desert may be sustained through a biogeophysical feedback mechanism [*Charney et al.*, 1975; *Zeng et al.*, 1999]. Changes of albedo and roughness from reduced vegetation cover could modify the net radiative flux at the surface and cause further desertification. Other processes, such as large scale circulation [*Wolter*, 1989], sea temperature [*Palmer*, 1986], ITCZ [*Greenhut*, 1981] associated with local meridional circulation change [*Liu et al.*, 2000], could affect the rainfall over the Sahara Desert.

Coupled ocean atmosphere models can simulate historical climate change and give some indications of future climate from increasing greenhouse gases [*Dai et al.*, 2000]. Using some observational and reanalysis data sources, the PCM 1.1 [*Washington et al.*, 2000] model is used to study the climate trends in the Sahara from the 1870s to the 2090s. From these data, 30-year mean climatology and trends of the Sahara Desert are similar in the twentieth century. The PCM simulates a drying, warming, shrinking, and northward retreating desert during the 21^{st} century.

Copyright 2001 by the American Geophysical Union.

Paper number 2001GL012883.
0094-8276/01/2001GL012883$05.00

2. Data and Definition

2.1 PCM 1.1 Outputs

PCM 1.1 has been used to simulate historical and future climate. The Historical Run (HR) is a ten-member ensemble starting from different months in 1870 and ending at December 1999. External forcing in HR, such as greenhouse gases is taken from observations. The Business As Usual Run (BAUR) for the external forcing is a linear extension of HR and consists of five members ranging from January 2000 to December 2099. The analyses are based on the whole member ensemble mean. A single Control Run (CR) will be used as a reference and it was integrated over 300 years with the 1990s condition as a perpetual.

2.2 Observational and Reanalysis Data

Observational and reanalysis data are used to evaluate the ability of PCM 1.1 to simulate the dry climatology and historical trend of the Sahara Desert. These sources include three 30-year 0.5°×0.5° climatological rainfall data sets from the Intergovernmental Panel on Climate Change (IPCC) [*New et al.*, 2000], 2.5°×2.5° NCEP/NCAR Reanalysis [*Kalnay et al.*, 1996], ECMWF Reanalysis (1979-93) and Xie and Arkin 2.5°×2.5° rainfall [*Xie and Arkin*, 1997].

2.3 Definition of the Sahara Desert

Several definitions of the Sahara Desert exist [*Tucker et al.*, 1991] and we define it as bounded by the 50 mm isoline of mean annual rainfall in the domain of 20°W~40°E longitude and 15°N~35°N latitude. We chose the 50 mm bound first because almost no vegetation cover exists inside and greenhouse effect might be an important factor to the potential change of the surface net radiative energy; and secondly all the data sources above show a better accordance than 200 mm defined by Tucker [1991] (Figure 1).

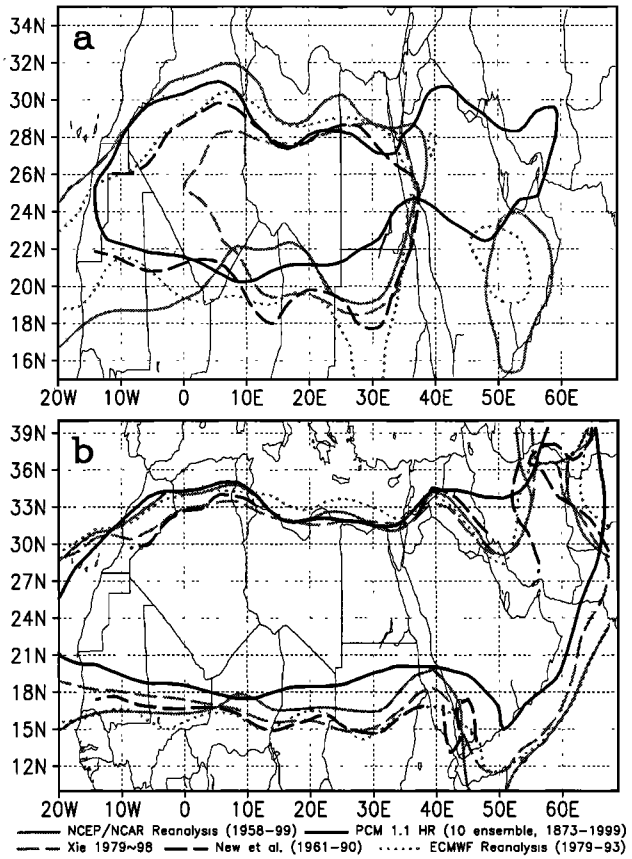

Figure 1. Climatological rainfall isolines of 50 (a) and 200 (b) mm covering the Sahara Desert from five data sources. Unit: mm/year.

3. Results

3.1. Climatology and Historical Trends

Isolines in figure 1a are 50 mm mean annual rainfall from the above sources which were all regridded into 2.8125° × 2.8125° linear grid resolution. The isolines correspond closely in all but the western boundary of the Xie isoline. In general, PCM 1.1 historical run follows that observed in the domain.

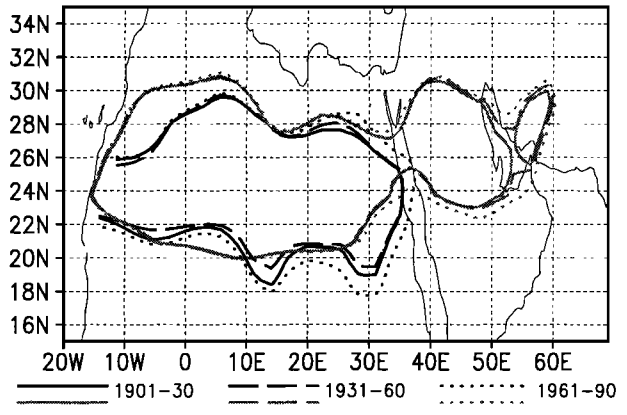

Figure 2. Trend of the Sahara in the 20^{th} century from New et al. (black) and PCM 1.1 HR (gray). Isolines are 30-year-mean 50 mm annual rainfall.

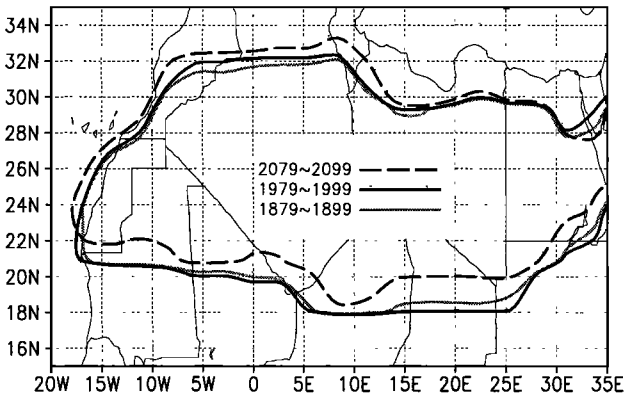

Figure 3. Trend of the Sahara bounded by last-20-year-mean 50 mm annual rainfall isoline from the 19^{th} to 21^{st} century simulated by the PCM 1.1.

For comparison, the regridded 200 mm isolines are shown in figure 1b. The five sources are very close to each other at the northern boundary but on the southern boundary, the PCM is mostly over 2° further north than the other sources. For this reason the 200 mm isoline was not chosen to represent the Sahara.

Trends of three 30-year climatology in figure 1 are selectively shown in Figure 2 with the PCM 1.1 as gray and IPCC as black. The isolines of 1901-30 and 1931-60 are coincident, which implies little change in the desert area. However, the 1961-90 solid isoline is about 1° further east and southward than those before and covers a larger area, enlarging the Desert similar to Tucker et al. [1991]. The dashed isolines overlay except a small southward shift at the southern boundary in 1961-90.

The PCM 1.1 HR in figure 1 and 2 has simulated reasonable dry climatology and 30-yr mean trend of the Sahara Desert in the twentieth century.

3.2. Future Trends

The CR and an ensemble average of HR and BAUR from PCM 1.1 are used to analyze trends in the Sahara Desert. The last-20-year mean of each century from 1879 to 2099 is shown in Figure 3 . The desert expands both at the southern and northern boundaries in 1979-1999 compared to 1879-1899. A much larger northward shift occurs in 2079-2099 at the southern boundary and leads to an apparent northward retreating trend and a size decreasing of the Desert.

Detailed trends of the whole Sahara average are shown in Figure 4 by 30-year running mean curves. The surface temperature and net radiative flux at the surface (NRFS) trends from CR (figure 4a and 4b) show a decadal change with a small amplitude. Trends of other fields from CR are similar (figures are not shown).

In the increasing greenhouse gases scenario, the curves in other panels of figure 4 show very different features from a and b. The size of Sahara, represented by the number of grid points (one grid box is approximately 95590 km^2) (figure 4c), grows throughout the 20^{th} century with a continuous increase from the 1950s to the 1990s. Such enlargement is in good agreement with Tucker [1991]. During the twenty-first century, the size decreases although the reference climatology of 1961-90 is in an enlarged period.

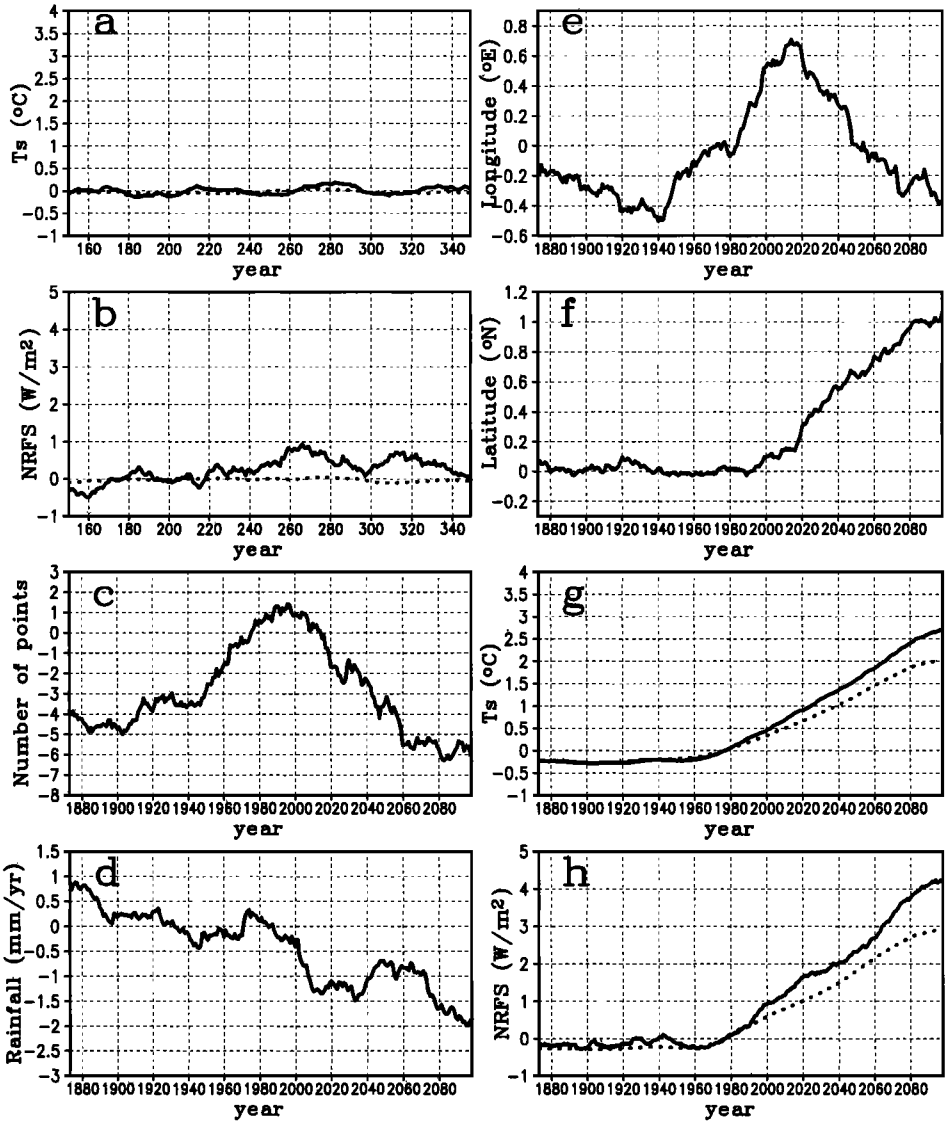

Figure 4. PCM 1.1 simulated 30-year running mean trends of the Sahara averaged as a whole. a, b are last 200-year deviation from CR and others are deviations from HR + BAUR relative to 1961-90 mean. Dotted lines in a, b, g and h are for global mean. a and g are surface temperature; b and h are net radiative flux at the surface. c,d, e and f are average number of grids, annual rainfall, longitude, and latitude respectively.

In the simulation the Sahara Desert becomes drier from the end of 19^{th} century to the 21^{st} (figure 4d), although the trend is not steady. In the end of 21^{st} century, the average rainfall is more than 2 mm/year less than 1961-90 mean.

Figure 4e and 4f show different trends in the latitudinal and meridional shifts. The east-west shift shows a centennial like change similar to the size trend. From the 1940s to the end of 2010, the Sahara moved eastward. After that, it retreated westward nearly to the same average longitude by the end of 2090 and in the 1940s. However, its meridional change appears to respond to the global warming trend. Before the 1990s, it stabilizes around the position of 1961-90 mean. It then moves steadily northward by the end of 2090s.

The global and local warming is shown in figure 4g. Before 1980s, both the solid (Sahara Desert) and doted (global) lines nearly stabilize to the 1961-90 mean. After that, the two lines become positive while the Sahara warms faster. By the end of 2090s, the Sahara is about 2.8°C warmer and the global mean is about 2°C more than the 1961-90 mean.

A direct cause of the warming trend could be that of NRFS (figure 4h). The positive trend of NRFS continues from the 1980s to the end of the 21^{st} century and it is over $+4W/m^2$ at last. The flux trend is almost the same as surface temperature (figure 4g). And it is opposite to the trend of that at the top of atmosphere found by Wiegner [1987]. From this point of view, the warming over the Sahara may be attributed to the local greenhouse effect.

4. Discussion

The warming trend over the Sahara Desert could be caused by a local greenhouse effect in a global greenhouse gases increasing background. The minimum low level meridional wind, which represents monsoon and ITCZ over the central Africa, unsteadily moves from 6.8°N in the 1870s to 6.4°N in the 1980s and then back to 6.8°N by the end of

2090s (figures not shown). Such trend is not so coincident to the northward retreating of the Sahara while the monsoon northward backing may cause the southern edge shrinking. The drying may relate to the water vapor budget trend over the Sahara column to which both local increase evaporation due to enhanced warming and processes in lower and higher latitudes may contribute. Much insightful investigation is necessary for such trends.

Acknowledgments. We are grateful to A. G. Dai and J. Arblaster for discussion and providing PCM output.

The research described is supported by the U.S. Department of Energy (DOE) Climate Change Prediction Program (CCPP), the Environmental Sciences Division Contract No. W-7405-Eng-48, the National Science Foundation (NSF) and the China National Key Programme for Developing Basic Sciences (G1998040900-part 1).

References

Bunting, A. H., Rainfall trends in the West African Sahel, *Q. J. Roy. Met. Soc., 102,* 59-64, 1976.

Charney, J., P. H. Stone, W. J. William, Drought in the Sahara: a biogeophysical feedback mechanism, *Science, 187,* 434-445, 1975.

Dai, A. G., T. M. L. Wigley, B. A. Boville, J. T. Kiehl, L. Buja, Climates of the 20^{th} and 21^{st} centuries simulated by the NCAR Climate System Model (CSM), *J. Clim.,* in press, 2000.

Dumont, H. J., Neolithic hyperarid period preceded the present climate of the central Sahel, *Nature, 274,* 356-358, 1978.

Gasse, F., R. Tehet, A. Durand, E. Gibert, J. G. Fontes, The arid-humid transition in the Sahara and the Sahel during the last deglaciation, *Nature, 346,* 141-146, 1990.

Greenhut, G. K., Comparison of temperature gradient model predictions with recent rainfall trends in the Sahel, *Mon. Wea. Rev., 109,* 137-147, 1981.

Kalnay, E., M. Kanamitsu, R. Kistler, W. Collins, D. Deaven, L. Gandin, M. Iredell, S. Saha, G. White, J. Woollen, Y. Zhu, A. Leetmaa, B. Reynolds, M. Chelliah, W. Ebisuzaki, W. Higgins, J. Janowiak, K. C. Mo, C. Ropelewski, J. Wang, Roy Jenne, Dennis Joseph, The NCEP/NCAR 40-year reanalysis project, *Bull. Am. Met. Soc., 77,* 437-471, 1996.

Klaus, D., Spatial distribution and periodicity of mean annual precipitation south of the Sahara, *Archiv fur Met., Geophy., und Biok., Ser. B, 26,* 17-27, 1978.

Littmann, T., Rainfall, temperature and dust storm anomalies in the African Sahel, *Geo. J., 157,* 136-160, 1991.

Liu, P., G. Wu, and S. Sun, Local meridional circulation and deserts, *Adv. Atm. Sci.,* accepted, 2000.

Maley, J., Palaeoclimates of central Sahara during the early Holocene, *Nature, 269,* 573-577, 1977.

New, M. G., M. Hulme and P. D. Jones, Representing twentieth century space-time variability. II: Development of a 1901-1996 mean monthly terrestrial climate fields, *J. Clim., 13,* 2217-2238, 2000.

Palmer, T. N., Influence of the Atlantic, Pacific, and Indian oceans on Sahel rainfall, *Nature, 322,* 251-253, 1986.

Ritchie, J. C., C. H. Eyles, and C. V. Haynes, Sediment and pollen evidence for an early to mid- Holocene humid period in the eastern Sahara, *Nature, 314,* 352-355, 1985.

Tucker, C. J., H. E. Dregne, and W. W. Newcomb, Expansion and concentration of the Sahara Desert from 1980 to 1990, *Science, 253,* 299-301, 1991.

Washington, W. M., J. W. Weatherly, G. A. Meehl, A. J. Semtner Jr., T. W. Bettge, A. P. Craig, W. G. Strand Jr., J. Arblaster, V. B. Wayland, R. James, and Y. Zhang, Parallel climate model (PCM) control and transient simulations, *Clim. Dyn., 16,* 755-774, 2000.

Wiegner, M., Determination of radiation balance at the upper edge of the atmosphere over the Sahara from satellite measurements, *Cologne, 38,* 9-39, 1987.

Wolter, K., Modes of tropical circulation, Southern Oscillation, and Sahel rainfall anomalies, *J. Clim., 2,* 149-172, 1989.

Xie, P. and P. A. Arkin, Global precipitation: a 17-year monthly analysis based on gauge observations, satellite estimates and numerical model outputs, *Bull. Am. Met. Soc., 78,* 2539-2558, 1997.

Zeng, N., J. D. Neelin, K.-M. Lau and J. Tucker, Enhancement of interdecadal climate variability in the Sahel by vegetation interaction, *Science, 286,* 1537-1540, 1999.

G. Wu and P. Liu, Laboratory of Atmospheric Sciences and Geophysical Fluid Dynamics, P.O. Box 9804, Beijing 100029, China. (e-mail: gxwu@lasg.iap.ac.cn, liup@lasg.iap.ac.cn)

G. A. Meehl and W. M. Washington, National Center for Atmospheric Research (NCAR), P.O. Box 3000, Boulder, CO 80307. (e-mail: meehl@ucar.edu; wmw@ucar.edu)

G. L. Potter, Program for Climate Model Diagnosis and Intercomparison, P.O. Box 808, L-264, Livermore, CA 94551-0808. (e-mail: gpotter@pcmdi.llnl.gov)

(Received January 21, 2001; accepted April 13, 2001.)